

Adsorption of Single Li and the Formation of Small Li Clusters on Graphene for the Anode of Lithium-Ion Batteries

Xiaofeng Fan,^{*,†} W. T. Zheng,[†] Jer-Lai Kuo,[‡] and David J. Singh^{*,§,||}

[†]College of Materials Science and Engineering and Key Laboratory of Automobile Materials of MOE, Jilin University, Changchun 130012, China

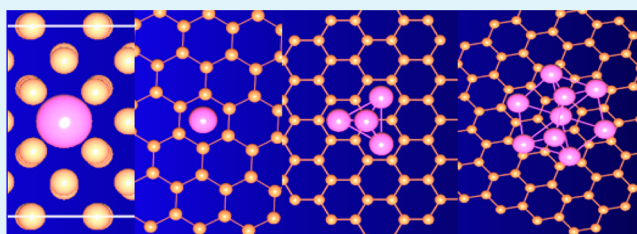
[‡]Institute of Atomic and Molecular Sciences, Academia Sinica, Taipei 10617, Taiwan

[§]Materials Science and Technology Division, Oak Ridge National Laboratory, Oak Ridge, Tennessee 37831-6056, United States

^{||}College of Materials Science and Engineering, Jilin University, Changchun 130012, China

ABSTRACT: We analyzed the adsorption of Li on graphene in the context of anodes for lithium-ion batteries (LIBs) using first-principles methods including van der Waals interactions. We found that although Li can reside on the surface of defect-free graphene under favorable conditions, the binding is much weaker than to graphite and the concentration on a graphene surface is not higher than in graphite. At low concentration, Li ions spread out on graphene because of Coulomb repulsion. With increased Li content, we found that small Li clusters can be formed on graphene. Although this result suggests that graphene nanosheets can conceivably have a higher ultimate Li capacity than graphite, it should be noted that such nanoclusters can potentially nucleate Li dendrites, leading to failure. The implications for nanostructured carbon anodes in batteries are discussed.

KEYWORDS: first-principles calculations, graphene, rechargeable lithium-ion batteries, adsorption of Li, formation of Li cluster



INTRODUCTION

Lithium-ion batteries (LIBs), although widely used, have certain shortcomings.¹ These include instabilities that can lead to battery failure under overcharging or overvoltage conditions and limits on capacity. Much theoretical and experimental work has focused on capacity, generally via modifications to the cathode or anode materials.^{2–4} Regarding the stability, there are at least two important factors: (1) the evolution of oxygen from the cathode, which can then react with the electrolyte⁵ and (2) the Li dendrite formation from the anode leading to failure of the separator layer.² Here, we focus on the anode. Carbon-based materials, particularly graphite and modified graphite, are used in practice. With graphite anodes, dendrite formation can be controlled. Since their introduction by the Sony Corporation in 1991,⁶ graphite and nongraphite carbon materials have always been important anode materials,^{7,8} although a lot of novel host lattices and lithium-metal alloys have been explored.² The theoretical capacity of graphite is limited to 372 mAh/g,⁹ but graphite anodes can be durable and avoid dendrite formation.¹

Graphene, with its single atomic-layer thickness, might be expected to have extra storage sites and therefore have a possibly higher capacity than graphite.^{10–15} Some experimental results have shown that graphene nanosheets and oxidized graphene nanoribbons can adsorb higher amounts of Li than graphite,^{16–18} for example, disordered graphene nanosheets with reported reversible capacities of 794–1054 mAh/g.¹⁷ However, on the basis of Raman spectra, Pollak et al. found that

pristine graphene has an evidently lower Li capacity than graphite.¹⁹ Moreover, it was reported on the basis of theory that Li cannot even reside on the surface of defect-free graphene in equilibrium with Li metal.²⁰ The conflicting experimental and theoretical results have motivated further study of Li adsorption on graphene.

Here, we explore the adsorption of Li atoms on graphene and the possibility that small Li clusters form on graphene using first-principles calculations. The Li–C interaction is analyzed in terms of the Li transfer between Li metal and graphene. We find that Li can be adsorbed effectively on defect-free graphene under favorable conditions. We further find that with increasing Li content, Li clusters can be formed on graphene nanosheets. This is because there is enough space between randomly arranged graphene nanosheets. These are potential nucleation centers for dendrite growth, which may become an issue with this type of anode. Therefore, although cluster formation may enable higher capacity, it poses stability issues.

THEORETICAL METHOD

The present calculations were performed with density functional theory using accurate frozen-core full-potential projector-augmented-wave (PAW) pseudopotentials and the VASP code.^{21–23} We used generalized gradient approximation (GGA) with the parametrization of Perdew–Burke–Ernzerhof (PBE)²⁴ and with added van der Waals

Received: April 26, 2013

Accepted: July 17, 2013

Published: July 17, 2013

(vdW) corrections for the surfaces. The k -space integrals and the plane-wave basis sets were chosen to ensure that the total energy is converged at the 1 meV/atom level. A plane wave expansion kinetic energy cutoff of 550 eV was found to be sufficient.

The calculated cohesive energy for bulk bcc Li is -1.61 eV with a lattice constant $a = 3.43$ Å. On the basis of calculations for graphite, we used a graphene primitive cell lattice parameter of 2.464 Å. The supercells were constructed with a vacuum space of 18 Å along the z direction. An 8×8 in-plane supercell with 128 carbon atoms was used to analyze the Li adsorption. The Brillouin zones were sampled using a Γ -centered $3 \times 3 \times 1$ k -point grid. The structures were fully relaxed, including both the lattice parameter and the positions of atoms. With Li adsorption, the change of the lattice constants was found to be very small and can be ignored. This is natural considering the stiffness of graphene. We did include dipole corrections for the potential and total energy as appropriate for the supercell geometry.

Previous theoretical studies showed that the interaction between Li and C is governed by charge transfer and that ionic bonding is the main interaction mechanism.^{25–27} However, we note that because of the large polarizability of graphene, the long-range vdW forces should also be considered to estimate accurately the strength of Li adsorption on graphene. Here, the effect of the dispersion interaction is included by the empirical correction scheme of Grimme (DFT + D/PBE), as implemented in the VASP code.²⁸ This approach has been successful in describing graphene-based structures.^{29,30} As shown in Figure 1a,

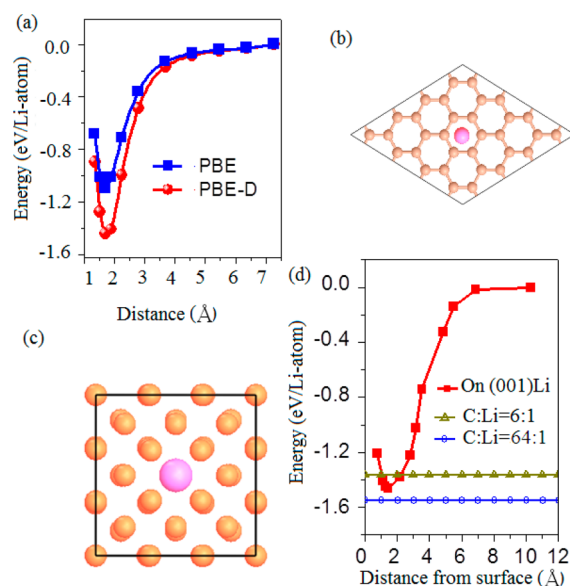


Figure 1. Potential energy surfaces and schematic representations of the structures of Li adsorbed on the center of the hexagonal carbon ring (a, b) and the (001) surface of the Li bulk (c, d).

for the equilibrium positions, the vdW forces make important contributions to the adsorption energy of Li on graphene. The long-range dispersion contribution to the adsorption energy is about 0.4 eV/Li, which is based on the 4×4 graphene model with adsorbed Li. This is consistent with previous theoretical results.³¹

RESULTS AND DISCUSSION

The discussion of the stability of an adsorbate system depends on the reference. The adsorption energy in studies of surface adsorption is usually defined to describe the stability of the adsorbate on some surface site via the formula $\Delta E_{ab} = E_{ab-surf} - E_{surf} - E_{ab}$, where $E_{ab-surf}$, E_{surf} , and E_{ab} are the total energy of the compound in which the adsorbate is adsorbed on the surface of the substrate, the isolated substrate with free surface, and the isolated adsorbate (i.e., a definition relative to free

adsorbate atoms), respectively. With this definition, Li can reside on the surface of defect-free graphene, as reported in previous studies.^{27,32–35} Among the different possible surface sites such as the midpoint of C–C bond (bridge) on top of a carbon atom (top) and the hexagonal center of a carbon ring (hex.), the latter is the most stable site. In the work of Lee et al.,²⁰ the interaction energy between Li and graphene is obtained with the formula, $\Delta E_{in}(x) = E(x) - E(0) - xE_{Li}$, where $E(x)$, $E(0)$, and E_{Li} are the total energy of the system per one formula unit Li_xC_6 , the isolated graphene with six carbon atoms, and one metallic Li atom in bulk Li. This is a better definition in the context of LIBs, as the formation of bulk Li represents anode failure and dendrite formation. (The interaction energy of Lee et al. is the formation energy in alloy theory that is used to estimate the stability of alloys against phase separation, which represents the stability against a Li-metal reservoir.) The calculated values of $\Delta E_{in}(x)$ are positive over entire range of the Li content from 0 to 1. This means there may be phase separation between Li and graphene (i.e., no adsorption). The difference between ΔE_{ab} and $\Delta E_{in}(x)$ is due to the different choice of the Li reference state. In the formula of ΔE_{ab} , the Li reference state is gas Li, and in the formula of $\Delta E_{in}(x)$, bulk Li is chosen as the reference state (note that the Li adsorption on graphene is an interface problem rather than a bulk alloy).

In experimental tests of electrode materials of LIBs, bulk Li is usually chosen as a reference electrode. In the test process, a Li ion is transferred from the surface of bulk Li to the tested anode materials. In an equilibrium situation, the appropriate reference is bulk Li and in that case, as mentioned, graphene does not adsorb Li. This is the case even when the extra stabilization from the van der Waals interaction is included. However, in an actual cell it is possible to have a kinetically limited process (i.e., there may be no available bulk Li reservoir or one may be concerned about the nucleation and growth of small Li particles). In fact, it is known that batteries can sometimes be operated beyond equilibrium stabilities, for example, because of the formation of protective interface layers. The analysis of such cases depends on the details. To proceed and examine whether graphene can store Li, we adopted a scenario that although optimistic may be still reasonable. Specifically, we used the adsorption energy of Li on the surface of bulk Li as the reference state to analyze the interaction between Li and graphene. Clearly, if the adsorption energy is positive with this reference, graphene will not be an effective anode material. As discussed below, even with this optimistic scenario we find problems with the use of graphene as an anode. In Figure 1c,d, we simulated the interaction between Li and the (001) surface of bulk Li. The most stable adsorption site is 1.44 Å from the surface (adsorption energy -1.463 eV/Li). For the $3^{1/2} \times 3^{1/2}$ supercell with a Li/C ratio of $1/6$, the adsorption energy of Li on graphene is -1.365 eV/Li. For the 8×8 supercell with two Li atoms where the Li/C ratio is $1/64$, the adsorption of Li is -1.55 eV/Li. In addition, it is found that the adsorption on both surfaces of graphene can not increase the binding energy when the Li content is lower than $1/6$. Therefore, Li can reside on the surface of pristine graphene in the context of LIBs, but the Li/C ratio on graphene should be less than $1/6$. This means that the amount of adsorbed Li is lower than for graphite even under this optimistic scenario. The reason is that both neighboring surfaces in graphite can aid Li adsorption through the vdW and Coulomb interactions.

Because the value of the formation energy $\Delta E_{\text{in}}(x)$ for the mixed system of Li and graphene is positive, it is possible that clusters of Li will be formed and phase separation will happen. In Figure 2, a pair of Li atoms adsorbed on graphene is studied

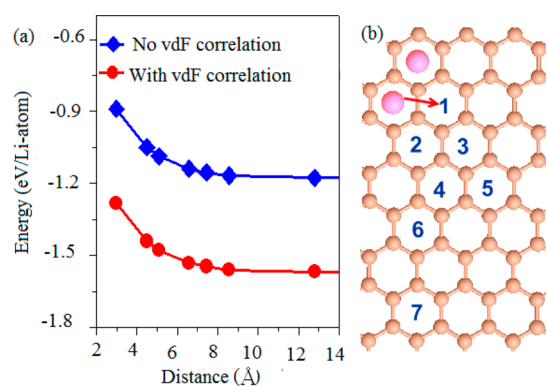


Figure 2. Adsorption energies (a) and schematic representations (b) for a pair of Li atoms adsorbed on graphene with different Li–Li distances. Note that the vdW correlation results in an increase in the adsorption energy (~ 0.4 eV/Li).

by simulation in an 8×8 supercell. We found that the energy of the system decreases as the pair's distance increases. This means that there is repulsion between the Li ions adsorbed on graphene. Coulomb repulsion is especially important when the pair of Li ions occupy the nearest-neighbor hexagonal sites. Therefore, in the low Li content regime, the Li ions will spread out on graphene.

Because the formation energy suggests phase separation, clusters of Li should be formed. For bulk Li, the binding energy is about 1.61 eV/Li. However, the binding energy of a small Li cluster is found to be markedly less than that of bulk Li. As shown in Figure 3a, the binding energy increases as the cluster size grows, as might be expected. For the larger-size cluster Li_{15} with 15 Li atoms (Figure 3b), the binding energy is about 1.03 eV/Li, which is still less than that of the surface Li atoms (1.463 eV/Li). Thus, the isolated small Li clusters are unstable in the presence of graphene or graphite because the Li atoms of a

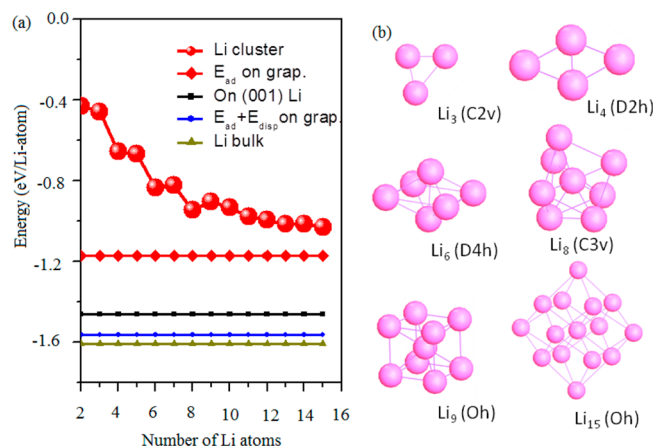


Figure 3. Cohesive energy of a Li atom in a Li cluster as a function of the number of Li atoms (a) and schematic representations of the clusters Li_3 , Li_4 , Li_6 , Li_8 , Li_9 , and Li_{15} (b). Note that E_{ad} and $E_{\text{ad}} + E_{\text{disp}}$ on grap. in panel a represents the adsorption energy without and with vdW correlation for a single Li adsorbed on graphene in an 8×8 supercell, respectively.

randomly formed cluster will be transferred to the surface of graphene or to the graphite.

On the basis of the above results, Li can be adsorbed on graphene when the concentration of Li is low. This leaves the question of what will happen as the Li concentration increases. One possibility is that the Li will congregate on the surface to form small clusters adsorbed on graphene. To address this, we analyzed the adsorption of Li clusters on graphene. First, we studied the different configurations of Li nanostructures adsorbed on graphene in detail. We found that Li clusters with certain sizes constitute the most stable state among the different configurations with the same Li concentration. As shown in Figure 4, we considered four adsorption config-

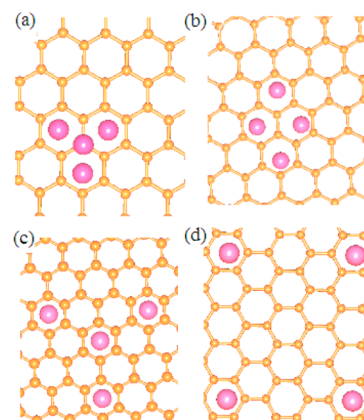


Figure 4. Schematic representations of the different Li-adsorption configurations on graphene, including cluster Li_4 (a), the plane structure (b), single Li adsorption with a short distance (c), and single Li adsorption with a large distance (d). Note that the results given are with 8×8 supercells with 128 carbon atoms. The adsorption energies (ΔE_{ab}) of panels a–d are -1.471 eV/Li, -1.365 eV/Li, -1.297 eV/Li, and -1.441 eV/Li, respectively.

urations on graphene. The Li_4 cluster is the most stable adsorption state. The adsorption energies decreases as the Li atoms are placed farther apart. However, at large separations, the adsorption energy increases. This is because at short-range there is a net attractive interaction between the Li resulting from effective metallic bonding that is related to the cluster stability (this also involves charge transfer to the graphene sheet), whereas at longer range there is a net screened Coulomb repulsion. We then analyzed the cohesive energy of a Li atom as a function of the number of Li atoms in the cluster (Figure 5). Here, the cohesive energy is defined by the formula, $\Delta E_c = (E_{\text{clu.-g}} - E_g - nE_{\text{Li}})/n$, where $E_{\text{clu.-g}}$ is the total energy of the compound in which Li clusters are adsorbed on graphene, E_g is that of the isolated graphene of an 8×8 supercell, E_{Li} is that of an isolated Li atom, and n is the number of Li atoms in the cluster adsorbed on graphene. It can be seen that the cohesive energy of Li atoms in clusters adsorbed on graphene is larger than the binding energy of Li atoms in the isolated cluster. This is due to the interaction between graphene and the Li ions of the Li cluster. In addition, the cohesive energy does not increase simply with the number of Li atoms in the cluster. Because of the limited local charge capacity of the graphene lattice, the localized charges transferred from Li ions just bind the ions with their nearest-neighbors. Therefore, increasing the number of Li ions will not result in an increase in the cohesive energy per Li. In the Li clusters, the Li ions above the Li ions on graphene (such as Li^2 of the Li_4 cluster in Figure

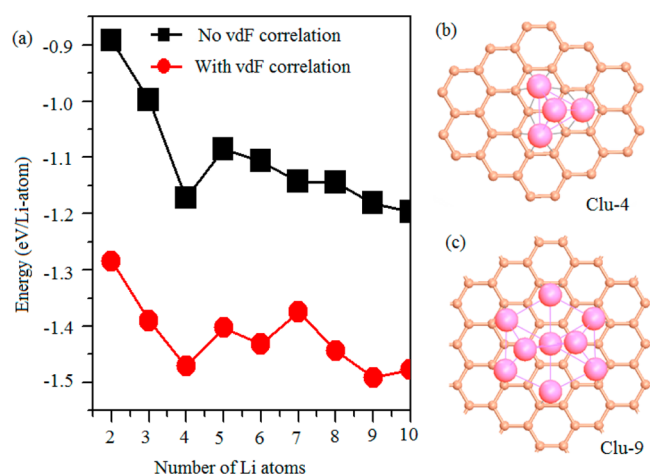


Figure 5. Cohesive energy (defined by $E_c = (E_{\text{clu-g}} - E_g - nE_{\text{Li}})/n$) of the Li atom as a function of the number of Li atoms for Li clusters adsorbed on graphene (a) and schematic representations of the clusters Li_4 (b) and Li_9 (c) adsorbed on graphene.

6d) can strongly bind their nearest-neighbor Li ions like that in Li metal. This can increase the cohesive energy. The fact that

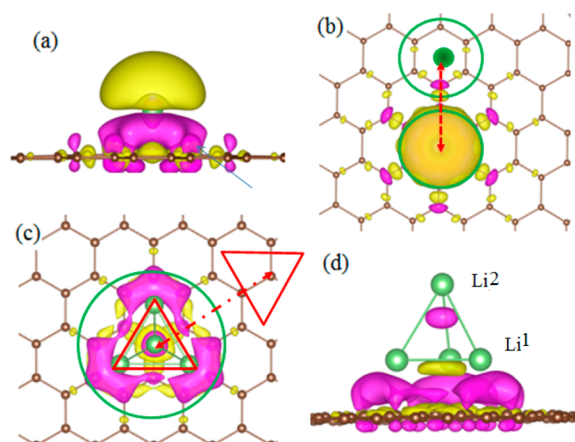


Figure 6. Three-dimensional charge-density redistribution calculated by the formula of charge-density difference for a single Li atom adsorption on graphene (a, b) and Li_4 cluster adsorbed on graphene (c, d). The isosurface levels are set at a negative value that is $1/4$ of the maximum negative value (yellow for charge depletion) and a positive value that is $1/6$ of the maximum positive value (magenta for charge accumulation).

the interaction between the above Li ions and graphene, including the Coulomb and vdW forces, is weak because of the long distance will reduce the cohesive energy. The vdW force in particular falls quickly with increased distance between Li and the graphene plane (Figure 1a). In addition, the shift of the Fermi level will decrease, and the interaction between Li ions and graphene has a weakening trend when the number of Li ions adsorbed on graphene is increased. Therefore, the cohesive energy does not simply increase. The next stable cluster adsorbed on graphene is Li_9 , whose cohesive energy is -1.491 eV/Li. The stable clusters Li_4 and Li_9 can be ascribed to special configurations. It is noted that the hex. site of graphene is the most stable site for Li adsorption. However, because of the interaction, the positions of the three Li ions on graphene deviate from this site (Figure 5b). With the introduction of other Li ions, the added Li ions will try to occupy the nearby

hex. site. However, the Li^2 ion (Figure 6d) cannot the bind these newly introduced Li ions. With the increase of the introduced Li ions, the interaction between Li ions will decrease the energy of system similar to that of the isolated Li clusters. However, with an increased number of Li ions, the number of Li^2 ions will increase. The net result is that Li_9 is stable when vdW interactions, which provide attraction between the Li^2 and the graphene, are included. For these stable adsorbed clusters, the adsorption energy is larger than that of the separated Li ions adsorbed on graphene with the same Li content. The calculated barriers for the Li-ion diffusion are 0.311 eV on graphene and 0.277 eV in graphite. The energy difference between the Li_2 cluster and two separated Li adsorbed on graphene is 0.28 eV. The energy difference between clusters differing in atom number by one, such as Li_2 and Li_3 , is less than 0.11 eV. Considering these energy scales, it is expected that Li_4 and Li_9 clusters can form in practice. Thus, we conclude that small Li clusters can be formed on graphene.

In previous research, it was found that Li adsorption does not significantly change the band structure of graphene. The charge transfer results in an up shift of the Fermi level, reflecting the electron count. In Figure 6, we analyzed the charge redistribution resulting from single Li adsorption as well as Li_4 cluster adsorption on graphene on the basis of the charge-density difference

$$\Delta CH(r) = CH_{\text{Li-g}}(r) - CH_{\text{Li}}(r) - CH_{\text{g}}(r)$$

where $CH_{\text{Li-g}}(r)$, $CH_{\text{g}}(r)$, and $CH_{\text{Li}}(r)$ are the real-space electronic charge distributions of the Li-adsorbed graphene, free graphene, and isolated Li, respectively. As seen in Figure 6a, the charge of Li is transferred to the region between Li and graphene. However, the charge from Li is kept in the local region under the Li ion because of the Coulomb interaction. Therefore, the Li ion that diffuses on the surface of graphene is not the simple naked Li^+ ion but is the screened Li ion with localized electronic charge. This reduces the Coulomb repulsion between Li ions. In addition, the charge of graphene is also redistributed to some extent. The charge congregates on the carbon atoms in the nearby region. It is seen that the charge is redistributed in the π antibonding state (π^*) of graphene. The charge is mostly distributed on the nearest-neighbor and next nearest-neighbor carbon atoms. Therefore, a nearest-neighbor Li ion can exist on the next nearest-neighbor hexagonal center, as shown in Figure 6b. This is because the graphene charge effectively screens the Li charge at this distance. The Li–Li distance is 4.27 Å, which is the explanation for the $1/6$ ratio of Li/C.

For the adsorption of the Li clusters, such as Li_4 in Figure 6c,d, the charge from the cluster is distributed at the local region under the cluster, which is similar to the case for single Li adsorption. In the Li_4 cluster, the Li–Li distance for the three Li atoms near graphene is 2.87 Å, and the distance between the Li^1 and Li^2 atoms (Figure 6d) is 3.07 Å. For bulk Li, the Li–Li distance is 2.97 Å. Therefore, the Li–Li distance of the Li_4 cluster adsorbed on graphene is very similar to that of bulk Li. The relative large distance between the Li^1 and Li^2 atoms may be ascribed to the charge accumulation in the center of Li_4 cluster. On the basis of the discussion about Li-pair adsorption, Li in groups of three should repel each other to some extent. Therefore, the fact that the Li_4 cluster is formed and adsorbed on graphene can be ascribed to the attractive effect of the Li^2 atom. Finally, we note that the formation of Li clusters on graphene does not have any obvious effect on the

band structure of graphene and results only in the up shift of the Fermi level similar to that of the single Li case.

CONCLUSIONS

We have studied the adsorption of Li atoms and Li clusters on graphene with first-principles calculations. We used Li surface energy as a reference and included van der Waals interactions. We found that the adsorption energy of Li on graphene is larger than the binding energy of Li on an (001) surface, although it is less than that of Li in Li metal. Therefore, under this optimistic assumption, Li can reside on the surface of defect-free graphene in the context of LIBs. In addition, it was found that the binding energy of Li in small isolated Li clusters is very small and therefore such isolated clusters are not stable in the environment of graphene. Although pairs of individual Li atoms on graphene have a repulsive interaction, we found that small Li clusters can be adsorbed on graphene. On the one hand, this means that relative to graphite one can envision conditions where more Li ions adhere to random-arranged graphene nanosheets (i.e., adsorption on the graphene surface plus the existence of vacancy and edges in the graphene nanostructures plus the adsorption of clusters). This may explain the results observed in the experimental tests of Li capacity. On the other hand, the much lower binding energies on pristine graphene and the formation of clusters imply issues with the stability of the anode against dendrite formation. Therefore, although a capacity increase using carbons with large amounts of graphene is conceivable, there may be stability issues with the use of such anodes, and the use of such anodes is unlikely to lead to increases in capacity in practical LIBs, at least without modifications.

AUTHOR INFORMATION

Corresponding Author

*E-mail: xffan@jlu.edu.cn (X.F.), singhdj@ornl.gov (D.J.S.).

Notes

The authors declare no competing financial interest.

REFERENCES

- (1) *Lithium Batteries: New Materials, Developments, and Perspective*; Pistoia, G., Ed.; Elsevier: New York, 1994.
- (2) Tarascon, J. M.; Armand, M. *Nature* **2001**, *414*, 359–367.
- (3) Whittingham, M. S. *Chem. Rev.* **2004**, *104*, 4271–4302.
- (4) Goodenough, J. B.; Kim, Y. *Chem. Mater.* **2009**, *22*, 587–603.
- (5) Edström, K.; Gustafsson, T.; Thomas, J. O. *Electrochim. Acta* **2004**, *50*, 397–403.
- (6) Nagura, T.; Tozawa, K. *Prog. Batteries Sol. Cells* **1990**, *9*, 209.
- (7) Noel, M.; Suryanarayanan, V. J. *Power Sources* **2002**, *111*, 193–209.
- (8) Burkhardt, S. E.; Bois, J.; Tarascon, J.-M.; Hennig, R. G.; Abruña, H. D. *Chem. Mater.* **2013**, *25*, 132–141.
- (9) Guerard, D.; Herold, A. *Carbon* **1975**, *13*, 337–345.
- (10) Lv, W.; Tang, D.-M.; He, Y.-B.; You, C.-H.; Shi, Z.-Q.; Chen, X.-C.; Chen, C.-M.; Hou, P.-X.; Liu, C.; Yang, Q.-H. *ACS Nano* **2009**, *3*, 3730–3736.
- (11) Yoo, E.; Kim, J.; Hosono, E.; Zhou, H.-S.; Kudo, T.; Honma, I. *Nano Lett.* **2008**, *8*, 2277–2282.
- (12) Jang, B. Z.; Liu, C.; Neff, D.; Yu, Z.; Wang, M. C.; Xiong, W.; Zhamu, A. *Nano Lett.* **2011**, *11*, 3785–3791.
- (13) Kaskhedikar, N. A.; Maier, J. *Adv. Mater.* **2009**, *21*, 2664–2680.
- (14) Liang, M.; Zhi, L. *J. Mater. Chem.* **2009**, *19*, 5871–5878.
- (15) Wu, Z.-S.; Ren, W.; Xu, L.; Li, F.; Cheng, H.-M. *ACS Nano* **2011**, *5*, 5463–5471.
- (16) Wang, G.; Shen, X.; Yao, J.; Park, J. *Carbon* **2009**, *47*, 2049–2053.
- (17) Pan, D.; Wang, S.; Zhao, B.; Wu, M.; Zhang, H.; Wang, Y.; Jiao, Z. *Chem. Mater.* **2009**, *21*, 3136–3142.
- (18) Bhardwaj, T.; Antic, A.; Pavan, B.; Barone, V.; Fahlman, B. D. *J. Am. Chem. Soc.* **2010**, *132*, 12556–12558.
- (19) Pollak, E.; Geng, B.; Jeon, K.-J.; Lucas, I. T.; Richardson, T. J.; Wang, F.; Kostecki, R. *Nano Lett.* **2010**, *10*, 3386–3388.
- (20) Lee, E.; Persson, K. A. *Nano Lett.* **2012**, *12*, 4624–4628.
- (21) Hohenberg, P.; Kohn, W. *Phys. Rev.* **1964**, *136*, B864–B781.
- (22) Kresse, G.; Furthmüller, J. *Phys. Rev. B* **1996**, *54*, 11169–11186.
- (23) Kresse, G.; Furthmüller, J. *Comput. Mater. Sci.* **1996**, *6*, 15–50.
- (24) Perdew, J. P.; Burke, K.; Ernzerhof, M. *Phys. Rev. Lett.* **1996**, *77*, 3865–3868.
- (25) Medeiros, P. V. C.; Mota, F. D.; Mascarenhas, A. J. S.; de Castilho, C. M. C. *Nanotechnology* **2010**, *21*, 115701.
- (26) Klintonberg, M.; Lebègue, S.; Katsnelson, M. I.; Eriksson, O. *Phys. Rev. B* **2010**, *81*, 085433-1–085433-5.
- (27) Fan, X.; Zheng, W. T.; Kuo, J.-L. *ACS Appl. Mater. Interfaces* **2012**, *4*, 2432–2438.
- (28) Grimme, S. *J. Comput. Chem.* **2006**, *27*, 1787–1799.
- (29) Fan, X. F.; Zheng, W. T.; Chihaiia, V.; Shen, Z. X.; Kuo, J.-L. *J. Phys.: Condens. Matter* **2012**, *24*, 305004.
- (30) Mercurio, G.; McNellis, E. R.; Martin, I.; Hagen, S.; Leysner, F.; Soubatch, S.; Meyer, J.; Wolf, M.; Tegeder, P.; Tautz, F. S.; Reuter, K. *Phys. Rev. Lett.* **2010**, *104*, 036102-1–036102-4.
- (31) Allouche, A.; Krstic, P. S. *Carbon* **2012**, *50*, 510–517.
- (32) Khantha, M.; Cordero, N. A.; Molina, L. M.; Alonso, J. A.; Girifalco, L. A. *Phys. Rev. B* **2004**, *70*, 125422-1–125422-8.
- (33) Martínez, J. I.; Cabria, I.; López, M. J.; Alonso, J. A. *J. Phys. Chem. C* **2008**, *113*, 939–941.
- (34) Garay-Tapia, A. M.; Romero, A. H.; Barone, V. J. *Chem. Theory Comput.* **2012**, *8*, 1064–1071.
- (35) Chan, K. T.; Neaton, J. B.; Cohen, M. L. *Phys. Rev. B* **2008**, *77*, 235430-1–235430-12.